AD-A250 832

DTIC
ELECTE
S MAY 2 8 1992
A D

Vector Analysis of Ice Fabric Data

Michael G. Ferrick and Kerran J. Claffey

March 1992

92-13962

92 5 27 035

For conversion of SI metric units to U.S./British customary units of measurement consult ASTM Standard E380, Metric Practice Guide, published by the American Society for Testing and Materials, 1916 Race St., Philadelphia, Pa. 19103.

COVER: Thin section of first-year sea ice with horizontal and aligned c-axes. (Photo by N. Perron.)

U.S. Army Corps
of Engineers
Cold Regions Research &
Engineering Laboratory

Vector Analysis of Ice Fabric Data

Michael G. Ferrick and Kerran J. Claffey   March 1992

Accesion For		
NTIS CRA&I		☑
DTIC TAB		☐
Unannounced		☐
Justification		
By		
Distribution /		
Availability Codes		
Dist	Avail and / or Special	
A-1		

PREFACE

Vector Analysis of Ice Fabric Data

MICHAEL G. FERRICK AND KERRAN J. CLAFFEY

INTRODUCTION

Environmental conditions at the time of ice forma-tion largely determine its structure. Ice crystals are uniaxial, and the optic axis corresponds to the c-axis. Random c-axis orientation is commonly observed near the top surface of newly formed sea ice in the Arctic. Once a cover has formed, the ice structure is characterized by long vertical columns that extend downward in the growth direction of the ice sheet, a result of quiescent, unidirectional growth. Under these conditions a selec-tive growth process occurs, and the c-axes of the crys-tals become primarily oriented in the horizontal plane of the ice sheet (Weeks and Ackley 1982). In the presence of a predominant current direction, strong c-axis align-ment develops in the direction of the current with generally decreasing scatter as ice thickness increases (Weeks and Gow 1978), and this ice structure causes anisotropic material behavior in all directions. Uniaxial compression data on first-year sea ice (Richter-Menge et al. 1987, Wang 1979) have indicated a strong depen-dence of peak compressive strength on c-axis alignment and on the angle between an applied load and the dominant c-axis direction. Therefore, to interpret data from mechanical property tests we must define the relative orientation and alignment of the ice fabric.

The techniques used in the analysis of ice fabrics were originally developed in structural petrology (see, for example, Fairbairn 1949, Knopf and Ingerson 1938, Turner and Weiss 1963). Crystal orientation measure-ments usually involve optical measurements of the c-axis orientations. Langway (1958) describes techniques for obtaining ice crystal c-axis orientation data using a Rigsby universal stage. One orientation measurement is made for each ice crystal in a sample, and these data are plotted on a Schmidt equal area net (Fig. 1) that represents a hemisphere of unit radius. The points on the net compose an orientation diagram that depicts the relative spatial concentration of the data, and this representation reduces, by one, the dimension of the hemisphere and of any plane or line. An orientation diagram may indicate a random or a patterned structure, depending on the dominant features of the diagram. A random fabric refers to a homogeneous distribution of the plotted points and represents an isotropic material. In this configuration there is an equal probability of finding points in equal area elements anywhere on the net. In contrast, the most significant feature of an anisotropic material is the preferred orientation indicated by the grouping of points on the net. A "girdle" corresponds to data that are distributed along a great circle of the net, indicating a preferred planar orientation of the c-axes. The pole of this great circle is termed the girdle axis. An area of highly concentrated data points (point maxi-mum) indicates a linear preferred orientation of the crystals in the fabric. The statistical significance of the orientation diagram increases if the main features (maxima/girdles) are reproducible in different compa-rable samples from the same homogeneous body.

Pearson (1901) used statistical arguments to develop the equation of a line or plane that provides the closest fit to points in space when all variables contain error. The solution depends on knowledge of the means, standard deviations, and correlations of the variables. A significant result was that the plane of best fit contains the line of best fit. Watson (1966) presented a matrix of sums of direction cosines of vectors representing crystal orientation in a Cartesian coordinate system. The rea-soning presented was that the greatest moment of inertia of the points would be about the eigenvector corre-sponding to the minimum eigenvalue of the matrix. Mardia (1972) used the same reasoning to obtain this matrix and interpret the results. Both Watson and Mardia propose distributions for the data on the sphere, and develop statistical analyses based on these assump-tions. Diggle and Fisher (1985) describe a program that computes these eigenvalues and eigenvectors and quan-titatively contours spherical data. The analysis of ice

fabric diagrams has been largely visual, frequently based on approximate data concentration contours drawn on the net. However, Herron and Langway (1982) applied the eigenvalue/eigenvector method of Mardia (1972) to study various fabric types, including small circle girdles and multi-maxima patterns. The results were interpreted qualitatively, and it was not clear whether any fabrics could be quantitatively assessed with this method.

In this report we seek a plane through the origin that minimizes the sum of the squared normal distances from the data, and obtain the dominant c-axis orientation in this plane. Beginning with the ice orientation data, a detailed derivation from simple geometric arguments is developed, yielding least-squares equations that minimize the orthogonal distance between the data

and a best line and plane. The eigenvalue problem that results is the same as that obtained by Pearson, Watson and Mardia. We identify an implicit assumption in this method of equal measurement uncertainty in each coordinate at all points on the sphere. Normalized eigenvalues provide quantitative measures of physical distance of the data from the plane and line, specifying the directional characteristics of the c-axes of crystals in a sample. Mean angular measures of variability are also developed. The development clearly indicates the fabrics that are well-described by the eigenvalue/eigenvector method, and provides a framework for developing related methods that may be useful for quantifying other fabric types. We demonstrate the capabilities of the analysis on data sets representing several samples of
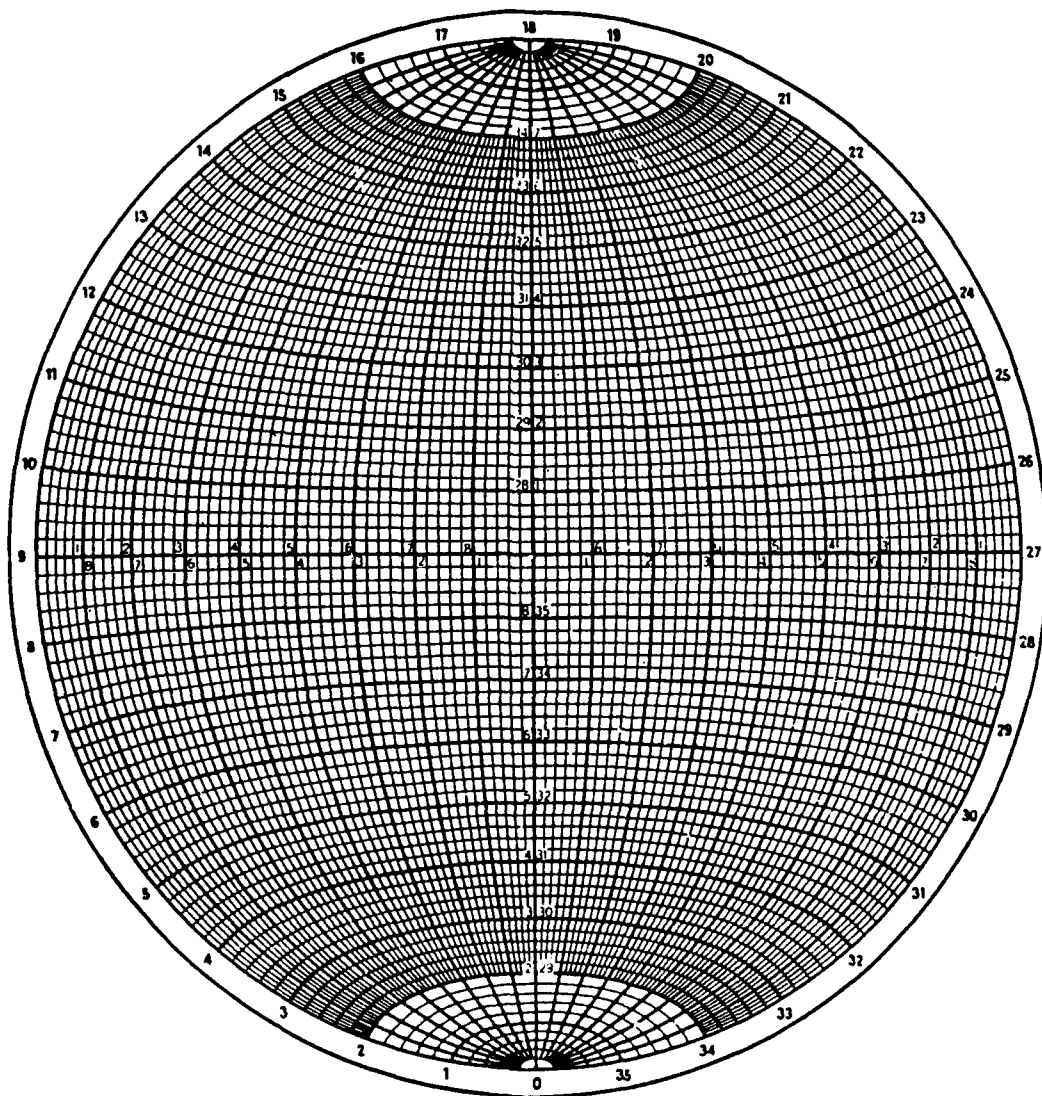

Figure 1. Schmidt equal area net.

2

first-year sea ice. The data and the results of the analysis are viewed on special Schmidt nets that represent data hemispheres defined by the best plane and the predominant basal plane, in addition to the xy-plane.

BACKGROUND

Measurement of the c-axis orientation of an ice crystal with a Rigsby universal stage provides an azimuth angle, an inclination angle, the direction of inclination as right or left, and the type of measurement as polar or equatorial. From these data we will obtain a pair of angles that define the orientation. The azimuth angle measures the rotation of the crystal about the z-axis that places the c-axis in the xz-plane. The zero azimuth can be chosen arbitrarily, depending on the requirements of the analysis. With the c-axis in the xz-plane, the inclination angle is the angle of tilt with the x-axis. An inclination angle of zero is defined as the angle where the c-axis of the crystal is parallel to the x-axis. It is found by rotating the crystal about the y-axis either to the right (clockwise) or the left (counterclockwise). The optic axis of a crystal can be aligned parallel to the z-axis, termed a polar measurement, or parallel to the x-axis, an equatorial measurement. The inclination angle measured with the Rigsby stage must be corrected for the optical error caused by the difference in the refractive indices of air and ice. The relationship between the corrected inclination, I, and the measured inclination, I_m, depends on the measurement type and can be expressed (Kamb 1962) as

$$I = \begin{cases} 1.04 \, I_m & \text{; equatorial} \\ \sin^{-1}\left(\frac{1}{1.31} \sin I_m\right) & \text{; polar} \end{cases} \tag{1}$$

Taken together, the azimuth and inclination measurements define the orientation of the optic axis of an ice crystal in three-dimensional space. The line representing each crystal in the sample is plotted through the origin of a sphere of unit radius. Each of these lines intersects the surface of the sphere at one point in each hemisphere. The surface of the lower hemisphere is traditionally represented in two dimensions with the Schmidt net (Fig. 1). The Schmidt net is also known as the equal-area net because a unit area in any position on the net corresponds to a unit area on the hemisphere. The crystal orientation data plotted on this net depict the relative spatial concentration of the measured data. The Schmidt net is composed of two sets of arcs. The set that crosses the x-axis represents the intersection of great circle planes passing through the y-axis with the unit sphere. These arcs are meridians of the net that correspond to inclination angles between −90° and +90°, representing the angle between the lower half of the yz-plane and the plane of the arc. The labels on the x-axis correspond to polar or equatorial crystal orientation with right or left tilt. The set of arcs that cross the y-axis are parallels of the net, and represent the intersection of planes parallel to the xz-plane with the sphere. The points of intersection of these arcs with the perimeter of the net represent the azimuth angle, and the notation on the net is in degrees of angle. Additional details that are needed for plotting crystal orientation data on the Schmidt net are given by Langway (1958).

DATA TRANSFORMATION TO CARTESIAN COORDINATES

Our analysis represents the c-axis of each ice crystal as a unit vector from the origin of a three-dimensional coordinate system in the half-space below the xy-plane, yielding an array of points on the surface of a hemisphere of unit radius. In this section we obtain three-dimensional Cartesian coordinates on the unit hemisphere (Fig. 2) for each crystal. The initial step in finding these Cartesian coordinates is to represent each point in spherical coordinates (ρ, θ, ϕ). Because each crystal is represented by a unit vector, the radius $\rho = 1$ for all the data. The angle θ, measured from the positive x-axis, is positive in the counterclockwise direction, and can be obtained from the measured azimuth Az as

$$\theta = \begin{cases} Az & \text{; polar-right, equatorial-left} \\ Az + 180° & \text{; polar-left, equatorial-right} \end{cases} \tag{2}$$

where Az is in degrees. Measurements made from the negative x-axis are adjusted by 180° in eq 2.

The angle ϕ is measured from the positive z-axis. The inclination angle was measured from the negative z-axis for polar crystals and from the xy-plane for equatorial crystals, and ϕ is determined as

$$\phi = \begin{cases} 180° - I & \text{; polar} \\ 90° + I & \text{; equatorial} \end{cases} \tag{3}$$

With the spherical coordinates specified, the equivalent Cartesian coordinates are obtained directly as

$$\begin{aligned} x &= \rho \sin\phi \cos\theta \\ y &= \rho \sin\phi \sin\theta \\ z &= \rho \cos\phi \end{aligned} \tag{4}$$
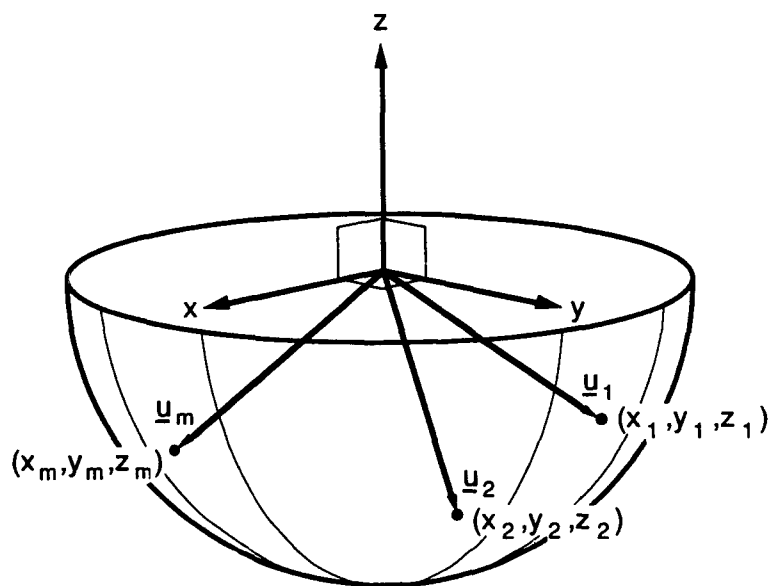
Figure 2. Sketch of unit vectors 1,2,...,m,...N representing the c-axis orientations of ice crystals in a sample. The hemisphere, z ≤ 0, is shown by convention.

MEASUREMENT ERRORS AND DATA FITTING

The relative uncertainties in x, y, and z caused by measurement error must be understood in order to identify an appropriate method for fitting the ice fabric data. Langway (1958) lists several sources of error in the measurement of c-axis orientation, and indicates that the errors in azimuth and inclination should each be less than 5°. Taking the errors in Az and I as random and of comparable magnitude, we observe from eq 2 and 3 that the same statement holds for errors in θ and ϕ. For an error of β in these angles we have from eq 4 that

$$x = \sin(\phi \pm \beta) \cos(\theta \pm \beta)$$
$$y = \sin(\phi \pm \beta) \sin(\theta \pm \beta) \quad (5)$$
$$z = \cos(\phi \pm \beta)$$

Expanding eq 5 and grouping terms according to the error we obtain

$$x = \sin\phi \cos\theta \cos^2\beta + \sin\beta \ (A \cos\beta + B \sin\beta)$$
$$y = \sin\phi \sin\theta \cos^2\beta + \sin\beta \ (C \cos\beta + D \sin\beta) \quad (6)$$
$$z = \cos\phi \qquad \cos\beta + \sin\beta \ (E)$$

where A, B, C, D, E are composed of sines and cosines of ϕ and θ. The relationships given in eq 4 are contained in eq 6, but they have been modified by errors of β. The

effect of measurement errors on the uncertainty in x, y, and z is variable. An error in θ only affects x and y. The resulting uncertainty in each coordinate is periodic, depending on θ, and out of phase with the other. The amplitude of these errors approaches zero near the pole and a maximum at the equator. Errors in ϕ affect all three Cartesian coordinates. The uncertainty in z is larger near the equator and smaller near the pole than the larger of x and y. Uncertainties in x and y resulting from errors in ϕ again vary individually with θ, displaying maximum amplitudes near the pole and approaching zero near the equator.

Classical least-squares methods require a dependent variable, but the coordinates of each c-axis are all independent. Reed (1989) presented a method for fitting a line to points in the plane when both coordinates of these points are independent and uncertain due to measurement error. The method allows the errors in the fit to be weighted according to the relative uncertainties in the measurement of x and y. The measurement errors discussed above could be considered by extending this method to three dimensions. However, we note for small β that $\cos\beta \approx \cos^2\beta \approx 1$ and $\sin\beta \approx 0$, indicating that errors in x, y, and z resulting from measurement errors are relatively small. As a first approximation we will choose equal weighting in each direction at every point, and the best fit line and plane will minimize the perpendicular distances from the data.

4

DETERMINATION OF THE BEST PLANE BY ORTHOGONAL LEAST-SQUARES

The unit vectors representing the c-axis orientation of each crystal in a sample have a common point at the origin of the unit sphere. The problem we consider in this section is to find the plane of best fit to fabric data that contains the origin, and to provide quantitative measures of the quality of the fit. The form of the equation of a plane through the origin is

$$f(x,y,z) = Ax + By + Cz = 0 \qquad (7)$$

We choose the function $F(x,y,z;c_1,c_2,c_3)$ with this same form and depending linearly on parameters c_1, c_2, c_3 as

$$F(x,y,z;c_1, c_2, c_3) = c_1\phi_1 + c_2\phi_2 + c_3\phi_3 = \sum_{i=1}^{3} c_i\phi_i = 0 \qquad (8)$$

where $\phi_1 = x, \phi_2 = y, \phi_3 = z$ are a specified set of mutually orthogonal functions and the c_i are unknowns to be determined. The pole of a plane is the point P of intersection with the hemisphere of a line normal to the plane through the origin. The unit normal n to the plane of best fit to the data has the form

$$\mathbf{n} = c_1 \mathbf{i}_1 + c_2 \mathbf{i}_2 + c_3 \mathbf{i}_3 = c_j \mathbf{i}_j \qquad (9)$$

where $\mathbf{i}_1$, $\mathbf{i}_2$ and $\mathbf{i}_3$ are unit vectors in the x, y and z directions, respectively, and repeated indices indicate summation.

A unit vector in 3-dimensional space represents each crystal in a sample, and the total number of crystals N used to fit the plane should be much larger than 3. For a data point m located at (x_m, y_m, z_m) we can evaluate $F(x_m, y_m, z_m; c_1, c_2, c_3) = F_m$ with eq 8 as

$$F_m = c_1 x_m + c_2 y_m + c_3 z_m \qquad (10)$$

The unit vector representing the c-axis of the mth crystal (Fig. 3) is

$$\mathbf{u}_m = x_m \mathbf{i}_1 + y_m \mathbf{i}_2 + z_m \mathbf{i}_3 = \phi_{1_m} \mathbf{i}_1 + \phi_{2_m} \mathbf{i}_2 + \phi_{3_m} \mathbf{i}_3 = \phi_{jm} \mathbf{i}_j \qquad (11)$$

The vector $\widetilde{\mathbf{w}}_m$ is the projection of $\mathbf{u}_m$ onto $\mathbf{n}$, representing the normal vector from the plane to the point (x_m, y_m, z_m)

$$\widetilde{\mathbf{w}}_m = (\mathbf{u}_m \cdot \mathbf{n})\mathbf{n} \qquad (12)$$

where $(\mathbf{u}_m \cdot \mathbf{n})$ is a scalar product between unit vectors. Throughout this development the notation (~) over a vector indicates that it does not have unit length. The normal distance d_m from point m to the plane is

$$d_m = (\mathbf{u}_m \cdot \mathbf{n}) = c_1 x_m + c_2 y_m + c_3 z_m \qquad (13)$$

and we observe that

$$|d_m| = |\widetilde{\mathbf{w}}_m| \leq 1 \qquad (14)$$

$$\widetilde{\mathbf{w}}_m = d_m \mathbf{n}$$

The sign of d_m distinguishes distances on opposite sides of the plane.

The orthogonal projection of $\mathbf{u}_m$ in the best fit plane is represented by the vector $\widetilde{\mathbf{v}}_m$, and
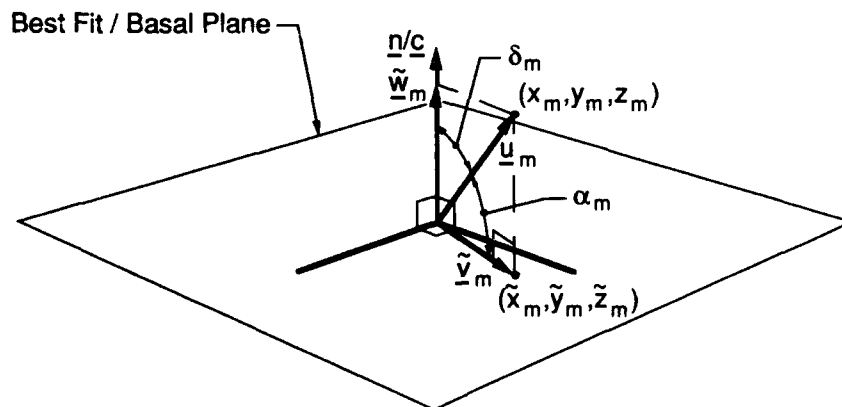
*Figure 3. Sketch of the unit vector $\mathbf{u}_m$ representing the mth crystal in an ice sample and its projections $\widetilde{\mathbf{v}}_m$ onto the best-fit plane or the basal plane, and $\widetilde{\mathbf{w}}_m$ onto $\mathbf{n}$ or $\mathbf{c}$ the unit normal vector to the corresponding plane. The angles between $\mathbf{u}_m$ and the best (plane, line) are (α_m, δ_m), respectively.*

$$\tilde{\mathbf{v}}_m = \mathbf{u}_m - \tilde{\mathbf{w}}_m = \tilde{x}_m \mathbf{i}_1 + \tilde{y}_m \mathbf{i}_2 + \tilde{z}_m \mathbf{i}_3 = \tilde{\phi}_{jm} \mathbf{i}_j \quad (15)$$

This vector joins the origin and the point $\tilde{x}_m, \tilde{y}_m, \tilde{z}_m$, the orthogonal projection of (x_m, y_m, z_m) in the plane. The vector $\tilde{\mathbf{v}}_m$ is unique and the best approximation of $\mathbf{u}_m$ in the plane. An equivalent statement is that the closest point in the plane to (x_m, y_m, z_m) is $\tilde{x}_m, \tilde{y}_m, \tilde{z}_m$. From eq 15 we can determine $\tilde{x}_m, \tilde{y}_m, \tilde{z}_m$ as

$$\begin{aligned}\tilde{x}_m &= x_m - d_m c_1 \\ \tilde{y}_m &= y_m - d_m c_2 \qquad \text{for } m = 1,2,...,N \quad (16) \\ \tilde{z}_m &= z_m - d_m c_3\end{aligned}$$

or

$$\tilde{\phi}_{im} = \phi_{im} - d_m c_i \qquad \text{for } i = 1,2,3 \quad (17)$$

where ϕ_{im} and $\tilde{\phi}_{jm}$ represent elements of N-dimensional vectors ϕ_i and ϕ_j, respectively.

We want to choose the c_i values that specify the plane through the origin with normal distances $|d_m|$ between the points representing the N crystals in a sample and the plane that are as small as possible. The N-vector $d = (d_1, d_2, ..., d_N)^T$ represents the individual normal distances from the data to the plane, where T indicates the transpose. Minimum normal distance to the plane is equivalent to maximum length of $\tilde{\mathbf{v}}_m$, the projection of $\mathbf{u}_m$ onto the plane. We will seek a least-squares fit and define E as a function of the unknown coefficients

$$E(c_1, c_2, c_3) = \sum_{m=1}^{N} |\tilde{\mathbf{v}}_m|^2 = \sum_{m=1}^{N} \sum_{i=1}^{3} \tilde{\phi}^2_{im} \quad (18)$$

Because we consider data projected onto a plane, the hemisphere in which the data appears is arbitrary. The sum of the squares of the lengths of $\tilde{\mathbf{v}}_m$ will be maximized and the sum of the squared distances from the plane d_m will be minimized where the gradient of E vanishes

$$\nabla E(c_1^*, c_2^*, c_3^*) = 0 \quad (19)$$

with c_i^* indicating coefficients of the plane of best fit.

We now perform the differentiation indicated in eq 19 with respect to c_j, where each choice of j yields a scalar equation of the form

$$\frac{\partial E}{\partial c_j} = 2\tilde{\phi}_{im} \frac{\partial \tilde{\phi}_{im}}{\partial c_j} = 0 \quad (20)$$

From eq 17 we obtain

$$\frac{\partial \tilde{\phi}_{im}}{\partial c_j} = -\left(d_m \delta_{ij} + c_i \frac{\partial d_m}{\partial c_j}\right) \quad (21)$$

where δ_{ij} is the Kronecker delta. We observe from eq 13 that $d_m = c_k \phi_{km}$, and differentiation of this equation yields

$$\frac{\partial d_m}{\partial c_j} = \phi_{km} \delta_{jk} = \phi_{jm} \quad (22)$$

Inserting eq 17, 21 and 22 into eq 20 we obtain the normal equations as

$$(\phi_{im} - d_m c_i)(d_m \delta_{ij} + c_i \phi_{jm}) = 0$$

or expanding and rearranging as

$$\phi_{jm} d_m \left(1 - c_i^2\right) + \phi_{im} \phi_{jm} c_i = d_m^2 c_j \quad (23)$$

Finally, because $\mathbf{n}$ is a unit vector and i is a summation index, $(1 - c_i^2) = 0$ and eq 23 becomes

$$\phi_{im} \phi_{jm} c_i = d_m^2 c_j \quad (24)$$

In eq 24 we observe that $d_m^2 = \lambda$, a constant, yielding an eigenvalue problem,

$$Ac = \lambda c \quad (25)$$

where each term a_{ij} of the 3×3 symmetric matrix A is

$$a_{ij} = \phi_{im} \phi_{jm} = \phi_i^T \cdot \phi_j \quad (26)$$

The eigenvalue λ is the sum of the squared normal distances of the data from the corresponding plane. Equation 25 in homogeneous form,

$$(A - \lambda I) c = 0, \quad (27)$$

indicates that nontrivial solutions exist if and only if

$$det(A - \lambda I) = 0 \quad (28)$$

The determinant given in eq 28 yields a cubic equation called the characteristic polynomial

$$\lambda^3 + p\lambda^2 + q\lambda + r = 0 \quad (29)$$

Following Beyer (1987) we obtain the solution as

$$\lambda = \begin{cases} m\cos\beta - p/3 \\ m\cos(\beta - 2\pi/3) - p/3 \\ m\cos(\beta - 4\pi/3) - p/3 \end{cases} \quad (30)$$

where

$$\beta = (1/3)\cos^{-1}\left(\frac{3b}{am}\right)$$

6

$$m = 2\sqrt{-a/3}$$
$$a = (1/3)(3q - p^2)$$
$$b = (1/27)(2p^3 - 9pq + 27r)$$

As p, q, and r are real, the eigenvalues will be real and distinct if

$$\frac{b^2}{4} + \frac{a^3}{27} < 0 \tag{31}$$

The spectral theorem (Shields 1968) states that because A is a real symmetric matrix it is similar to a diagonal matrix B composed of the eigenvalues of A, and therefore the eigenvalues of A are real. Similar matrices have the same trace and the same determinant. The trace of a matrix is the sum of the elements on the principal diagonal. The elements a_{11}, a_{22} and a_{33} of matrix A represent the sum of the squares of the distances between the data and the three planes defined by the coordinate axes. As each crystal is represented by a unit vector,

$$tr(A) = \sum_{i=1}^{3} a_{ii} = N = tr(B) = \sum_{i=1}^{3} b_{ii} = \sum_{i=1}^{3} \lambda_i \tag{32}$$

indicating that the sum of the eigenvalues is N, the total number of crystals in the sample. The determinants of A and B are the product of the eigenvalues. The eigenvalues of A are nonnegative if A is positive semidefinite, that is, $x^T A x \geq 0$ for any x. Large diagonal elements relative to those off the main diagonal are characteristic of a positive semidefinite matrix. Since the eigenvalues represent sums of squared distances, $\lambda_i \geq 0$ and matrix A is positive semi-definite. We will designate the eigenvalues in increasing order according to magnitude as $\lambda_1 \leq \lambda_2 \leq \lambda_3$, and define normalized eigenvalues as

$$\lambda_i' = \frac{\lambda_i}{N} \tag{33}$$

The normalized eigenvalues give the mean squared normal distance between the points on the unit sphere defined by the c-axis vector of the individual crystals and the plane normal to the corresponding eigenvector. These eigenvalues provide a measure of the fit that is equivalent to the variance in classical dependent variable least-squares methods.

Eigenvectors of a real symmetric matrix corresponding to different eigenvalues are orthogonal, and because the eigenvalues are real, the eigenvectors can be taken to be real. The vector v is an eigenvector for A belonging to the eigenvalue λ if

$$Av = \lambda v \quad \text{and} \quad v \neq 0 \tag{34}$$

The lengths of these eigenvectors are arbitrary, and we normalize them to unit length to obtain an orthonormal basis in three-dimensional space. Each eigenvector represents the unit normal to a plane, and the corresponding eigenvalue gives the sum of the squared normal deviations of the data from that plane. The minimum eigenvalue defines the plane of best least-squares fit to the data, and the higher eigenvalues are associated with the remaining mutually orthogonal planes through the origin. With the origin fixed, the eigenvector basis represents a coordinate system that is rotated relative to the coordinate axes.

The eigenvectors written in columns form the matrix P. The elements of P are the direction cosines between each eigenvector and the coordinate axes. The angle α_{ij} between the eigenvector v_j and the axis i_i is

$$\alpha_{ij} = \cos^{-1}(v_j \cdot i_i) = \cos^{-1}(p_{ij}) \tag{35}$$

Because the columns of P are orthonormal, P is an orthogonal matrix, $P^{-1} = P^T$ is also orthogonal, and $det\,P = \pm 1$. Matrices A and B are related through P as

$$A = PBP^T \tag{36}$$

representing a singular value decomposition of A. The diagonal elements of B are the singular values σ_i as well as the eigenvalues of A. With singular values ordered by their magnitude in the same way as the eigenvalues, the condition number of matrix A of full rank is

$$\text{cond}(A) = \frac{\sigma_3}{\sigma_1} = \frac{\lambda_3}{\lambda_1} \tag{37}$$

Condition numbers $>>1$ indicate that A is nearly singular.

The sum of the squared normal distances between the data and the best plane, given by λ_1, provides a measure of the planar structure of an ice sample. Values of λ_1 or λ_1' approaching zero indicate an increasingly planar ice structure. If $\lambda_1 = 0$, then cond(A) $= \infty$ and the data are perfectly planar. A visual representation of the error is obtained from the angle α_m between an individual crystal and its projection in the best plane (Fig. 3).

$$\alpha_m = |\pi/2 - \cos^{-1}(u_m \cdot n)| \tag{38}$$

The absolute value in eq 38 is needed if the angle between u_m and n is greater than $\pi/2$. The average angular deviation $\bar{\alpha}$ between the data and the best plane is a parameter we term the planar spread that can be readily determined and understood:

$$\bar{\alpha} = \frac{1}{N} \sum_{m=1}^{N} \alpha_m \tag{39}$$

7

A small planar spread indicates a small mean angle between the crystals in a sample and the plane.

DEVELOPMENT OF DEPENDENT VARIABLE LEAST-SQUARES SOLUTIONS

We will now parallel the development of the previous section to obtain a set of classical dependent variable least-squares solutions to the problem of fitting a plane to three-dimensional data. This standard method seeks a minimum error in the dependent variable and is more commonly available than the orthogonal method, but the results are sensitive to the choice of dependent variable. Arbitrarily selecting z as the dependent variable, we rewrite eq 8 as

$$z = F(x,y) = c_1 \phi_1 + c_2 \phi_2 \tag{40}$$

where $\phi_1 = x$ and $\phi_2 = y$. The coefficients c_1 and c_2 are chosen so that the deviations d_m are as small as possible,

$$d_m = r_m - F(x_m, y_m; c_1, c_2), \tag{41}$$

in which r_m is z_m, the z-value of the mth point, and $F(x_m, y_m; c_1, c_2)$ is the corresponding z-value in the plane of best fit. Again, the vector d contains all the deviations d_m, and we seek a least-squares fit to the data with

$$E(c_1, c_2) = \sum_{m=1}^{N} \left[r_m - F\left(x_m, y_m; c_1, c_2\right) \right]^2 \tag{42}$$

Taking the gradient of E and setting it to zero yields the normal equations

$$\sum_{m=1}^{N} \left[r_m - F\left(x_m, y_m; c_1, c_2\right) \right] \phi_{im} = 0, \quad i = 1,2 \tag{43}$$

or

$$d^T \cdot \phi_i = 0$$

indicating that the vector of deviations is normal to each vector ϕ_i. Now, inserting eq 40 and rewriting the normal equations in vector form we obtain a pair of linear equations:

$$\left[\phi_j^T \cdot \phi_i \right] c_j = r^T \cdot \phi_i \qquad i = 1,2 \tag{44}$$

The vector normal to the plane that minimizes the sum of the squared z-distances with the data is

$$\tilde{n} = c_1 i_1 + c_2 i_2 - i_3$$

or in the form of a unit vector,

$$n = \frac{1}{\left(c_1^2 + c_2^2 + 1\right)^{1/2}} \left(c_1 i_1 + c_2 i_2 - i_3\right) \tag{45}$$

The normal distances between the data and the plane represented by n can then be determined using eq 13 as

$$|\tilde{w}_m| = (u_m \cdot n) = \frac{\left(c_1 x_m + c_2 y_m - z_m\right)}{\left(c_1^2 + c_2^2 + 1\right)^{1/2}} \tag{46}$$

for $m = 1, 2, \ldots, N$

The sum of the squared normal distances given in eq 46 is the same measure as the minimum eigenvalue obtained in the previous section. The planes that minimize the squared x-deviations and squared y-deviations are obtained by interchanging the roles of ϕ_1, ϕ_2 and r above, and repeating the analysis.

ALIGNMENT OF THE C-AXES

An area of highly concentrated c-axis data on the Schmidt net indicates a linear preferred orientation of the ice crystals of a sample, and suggests the need to determine the predominant optic axis orientation of the fabric. We will locate this linear orientation by following a development parallel to that used to determine the best plane. The unit vector c represents the unknown preferred c-axis orientation of the crystals in a sample, and is expressed as

$$c = c_1' i_1 + c_2' i_2 + c_3' i_3 \tag{47}$$

where the primes distinguish these coefficients from those of the unit vector n given in eq 10. The plane through the origin that is normal to c represents the predominant basal plane orientation of the crystals in the sample and is described by

$$F\left(x,y,z; c_1', c_2', c_3'\right) = c_1' x + c_2' y + c_3' z = 0 \tag{48}$$

As before, the unit vector u_m represents the mth crystal orientation and intersects the unit hemisphere at (x_m, y_m, z_m). In order to take advantage of the detail given in the previous development, the vector projections of u_m onto the plane and its normal vector are again $\tilde{v}_m$ and $\tilde{w}_m$, respectively. Then, with c replacing n and a different normal plane, Figure 3 represents our present condition.

When searching for the best plane we sought to minimize the squared normal distance $|\tilde{w}_m|$. However, the closest representation of u_m by the unit vector c

8
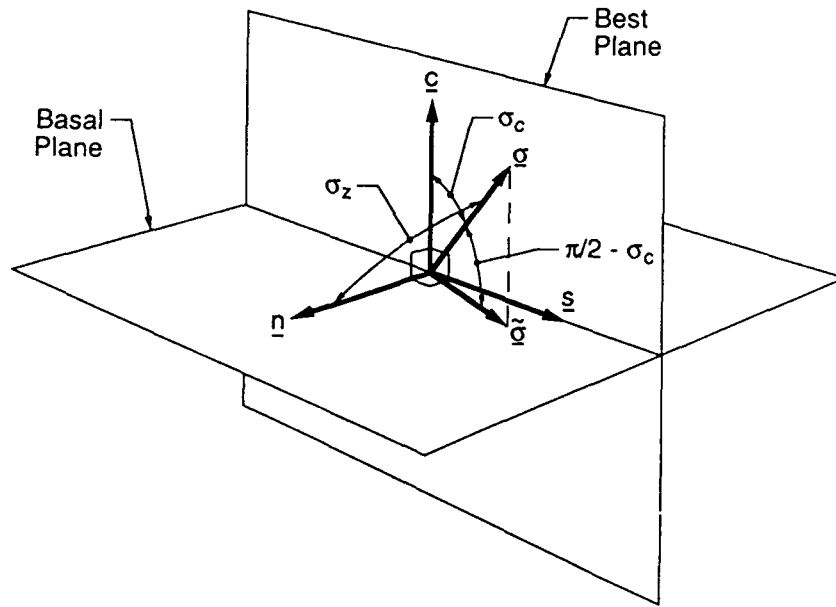
*Figure 4. Unit vector **c** representing the linear preferred c-axis orientation of the ice fabric, and the long axis of the columnar crystals of an ice sample are represented by **n**. The unit vectors **n** and **s** provide the predominant orientation of the basal plane of the sample. A unit vector **σ** represents the direction of load application on the sample, $\tilde{\sigma}$ is the projection of this vector onto the basal plane, σ_c is the angle between the applied load and **c**, and σ_z is the angle between the load and **n**.*

requires that we maximize the sum of the squares of the lengths of $\tilde{w}_m$. The predominant basal plane orientation is then the plane of maximum squared normal error with the data. Each step in the previous development applies except that c_i is replaced by c'_i. Note that the matrix A given in eq 26 is unchanged because it depends only on the coefficients of the intersections of the individual unit vectors u_m with the unit hemisphere. Therefore, we are solving the same eigenvalue problem as before. The eigenvectors obtained in eq 34 are orthogonal, and **c** is contained in the best plane. Kass (1989) has shown for the general case that spaces of closest fit are nested. Every p-dimensional subspace of closest fit lies in one of dimension $p + 1$. The third eigenvectors together with **c** form the plane of best fit to the c-axes, and **s** and **n** form the predominant basal plane (Fig. 4). The direction cosines of the angles between the preferred linear orientation and the coordinate axes are given in matrix P, and the angles can be obtained from eq 35.

The mean squared normal distance between the data and the vector **c** is $\lambda'_1 + \lambda'_2$ or $1 - \lambda'_3$. Again using angles to visualize error, the angle δ_m between an individual (crystal) vector and its projection onto **c** (Fig. 3) is obtained as

$$\delta_m = \cos^{-1}\left(u_m \cdot c\right) \tag{49}$$

Linear spread between these vectors is always $\leq 90°$. If δ_m obtained with eq 49 is $> 90°$, δ_m is replaced by its supplement. The average angle $\bar{\delta}$ between the data and **c** is

$$\bar{\delta} = \frac{1}{N} \sum_{m=1}^{N} \delta_m \tag{50}$$

The parameter $\bar{\delta}$ is termed the linear spread, and a small $\bar{\delta}$ indicates that the angles between the preferred orientation and the data are also small.

As a group, the eigenvalues provide measures of the structure of the ice sample. An eigenvalue of zero occurs if the data are 2-dimensional, and a pair of zero eigenvalues represent 1-dimensional data. More generally, small $\lambda'_1 \approx \lambda'_2$ together with large λ'_3 occurs with aligned data, and small λ'_1 with significantly larger λ'_2 and λ'_3 indicates planar data. If in addition to small λ'_1, $\lambda'_2 \approx \lambda'_3$ the crystal orientations distribute symmetrically about a great circle of the sphere. With $\lambda'_1 = \lambda'_2 = \lambda'_3$ every set of orthonormal vectors will serve as the eigenvectors. The data are maximally dispersed with respect to lines and planes, and the material is isotropic.

If the c-axes in a given sample are sufficiently aligned, the mechanical properties of the ice will be affected. If **σ** is a unit vector in the direction of an applied force, the angle σ_c between the force and the

9

dominant c-axis direction is

$$\sigma_c = \cos^{-1} (\sigma \cdot c) \tag{51}$$

and the complement of σ_c is the angle between the load and the basal plane (Fig. 4). For a columnar ice sample n gives the predominant direction of crystal elongation and growth. The angle σ_z between the load and the vector n is obtained as

$$\sigma_z = \cos^{-1} (\sigma \cdot n) \tag{52}$$

SCHMIDT NET REPRESENTATIONS

The results of the analysis of an ice sample are presented together with the data on the Schmidt net. The initial step in finding the Cartesian net coordinates is to obtain polar coordinates (r,θ) on the net for each point. The polar angle θ on the net is the same as the spherical angle θ given in eq 2. The spherical angle ϕ given in eq 3 is used to find the radial coordinate. The supplement of ϕ, measured from the negative z-axis, has the same sine as ϕ, and the distance from the origin of the Schmidt net r is (Knopf and Ingerson 1938)

$$r = (2a)\sin(\phi/2) \tag{53}$$

where $a = 0.70711R$, and R is the radius of the net. The equivalent Cartesian coordinates are then obtained directly as

$$x = r\cos\theta$$
$$\tag{54}$$
$$y = r\sin\theta$$

Planes that pass through the origin intersect the unit sphere as a great circle. The part of the great circle of the best fit plane below the xy-plane is drawn on the Schmidt net. With $\rho = 1$, eq 4 is substituted into eq 8 and solved for ϕ to obtain

$$\phi = \tan^{-1} \left(\frac{-c_3}{c_1 \cos\theta + c_2 \sin\theta} \right) \tag{55}$$

where θ is incremented in arbitrary steps from $0°$ to $360°$. The requirement of $z \leq 0$ in eq 4 identifies the points of intersection in the lower hemisphere. We obtain polar coordinates on the net from these spherical coordinates, and then eq 54 yields a discrete representation in Cartesian coordinates of the great circle on the net. Experience indicates that $0.5°$ increments of θ yield a smooth curve on the net.

The unit normal n to the plane of best fit from the

origin is the pole vector. It intersects the unit hemisphere at the pole point P with coordinates (x_p, y_p, z_p) or (c_1^*, c_2^*, c_3^*). Inverting eq 4 we obtain the spherical coordinates of this point as

$$\phi = \cos^{-1} (c_3) \tag{56}$$

$$\theta = \tan^{-1} \left(\frac{c_2}{c_1} \right)$$

There are two values of θ in the range $0° \leq \theta < 360°$ that have the same tangent. If the value of $x = c_1$ is negative, θ falls in the 2nd or 3rd quadrant and the calculated angle is adjusted by adding $180°$. Again, the polar coordinate r on the net is obtained from eq 53, and the Cartesian coordinates of the pole on the net are found from eq 54. The determination of the Schmidt net coordinates of c, representing the intersection of the preferred linear orientation and the unit hemisphere, follows the same procedure as for the pole vector with (c_1, c_2, c_3) in eq 56 replaced by (c_1', c_2', c_3'). The intercept of the linear orientation vector must fall on that of the great circle of best planar fit.

During field ice coring and thin section preparation, a sample intended as horizontal may deviate by an angle of several degrees. Sea ice with horizontal c-axis alignment will then be represented by a best plane at this angle. The linear dimensions on the periphery of the Schmidt net are distorted, and it is difficult to judge normal distances between the data in this region and the trace of the best plane. Points that appear near the perimeter and directly across the net from each other represent crystals with close planar alignment. For these reasons it is frequently advantageous to view the data on Schmidt nets drawn on alternative planes. Viewing the data on a Schmidt net drawn in the best fit plane with n vertical eliminates sample preparation error for horizontally aligned sea ice. The great circle of the best plane falls on the perimeter of the net and the pole of this plane appears at the origin. With c vertical the plane of the Schmidt net is the predominant basal plane of the sample, and the data are transformed from the perimeter to the middle of the net. The great circle of the plane of best fit then must pass through the origin. Accurate visual assessments of the linear and planar preferred orientations of the sample are possible on this net because of minimal distortion of linear distance near the origin. With these planes for mapping, the importance of net distortion, sample preparation, and measurement accuracy are minimized by providing optimal views of the crystal fabric.

Unit vectors in the Cartesian coordinate directions were used in eq 11 to obtain a unit vector representing each crystal in a sample. These unit vectors are related to an orthogonal coordinate system of eigenvectors

10
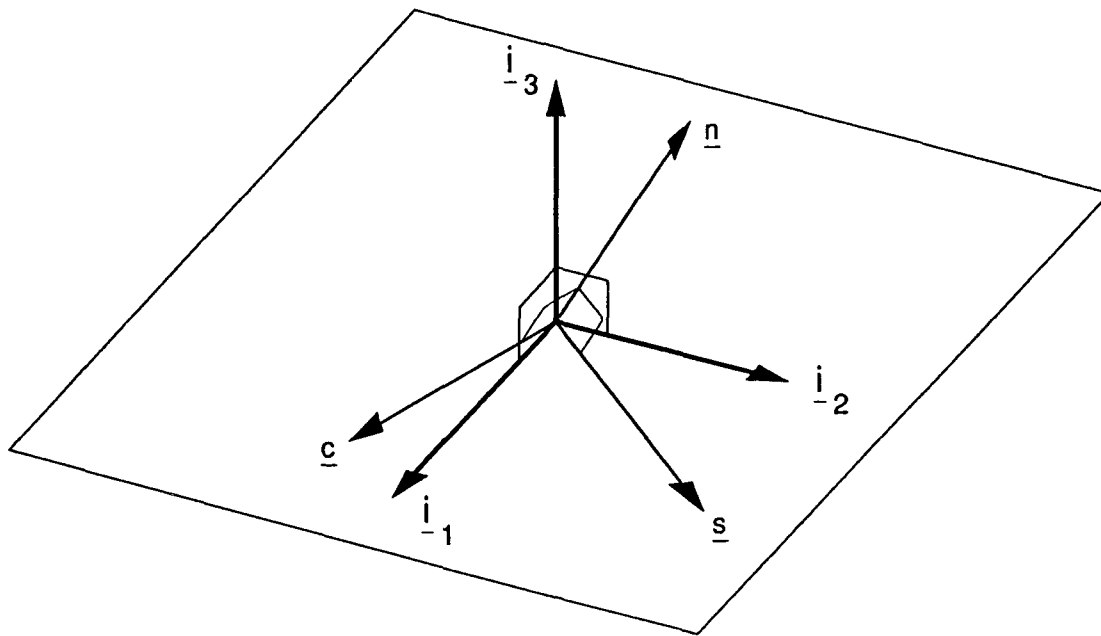
Figure 5. Relationship between the Cartesian and eigenvector coordinate systems for visualizing alternate Schmidt net representations of ice fabric data.

$\left(i'_1, i'_2, i'_3\right)$ by the matrix P as

$$i'_j = p_{ij} i_i \qquad (57)$$

This relationship is depicted in Figure 5 with eigenvectors **n**, **c**, and **s** as the (primed) unit eigenvectors. The relationship between a general vector in the Cartesian system and its transform in the eigenvector system is (Hildebrand 1965)

$$u'_m = P^{-1} u_m = P^T u_m \qquad (58)$$

and P is termed the transformation matrix. Because P is orthogonal, transformations using P are orthogonal. Orthogonal transformations maintain length and preserve angle, and can be interpreted as a combination of rotations and reflections. The order of the eigenvector placement in P determines the transformation, and either **n** or **c** is made vertical.

APPLICATIONS

We analyzed the ice fabric of many samples of first-year sea ice taken from the Beaufort Sea. Both orthogonal and dependent variable least-squares analyses were used and compared. These cases are presented in Figure 6 in an arbitrary order from highest to lowest mean normal error of the best plane obtained from the or-thogonal analysis. In all cases this approach provided a lower bound to the normal error of the dependent variable methods. The individual samples are designated by the dependent variable analysis with mean normal error closest to that of the orthogonal analysis. The dashed lines connecting the mean normal errors for the dependent variable solutions are erratic. Different dependent variable choices produced dramatically different planes with widely varying normal errors. The coordinate axis most nearly normal to the plane of the data provided the lowest mean error. Diminishing mean normal error generally corresponds to diminishing planar spread. However, the minimizations of these two parameters are not equivalent, explaining the lack of perfect agreement between the trends plotted in Figure 6. The mean normal errors for most of these cases are less than 0.1, corresponding to planar spreads of less than 12°. These results indicate that these samples have planar fabrics.

The same cases were also analyzed for preferred alignment of the c-axes. Mean squared normal distance between the data and the best vector **c** is $1 - \lambda'_3$. The maximum normalized eigenvalue and the linear spread are displayed in Figure 7. Values of λ'_3 that exceed 0.9 correspond to linear spreads of less than 15°. Linear spread is larger than planar spread because it represents angles with a particular line in the plane, while planar spread represents angles with the plane itself. Comparing Figures 6 and 7 we observe that increasingly planar

11
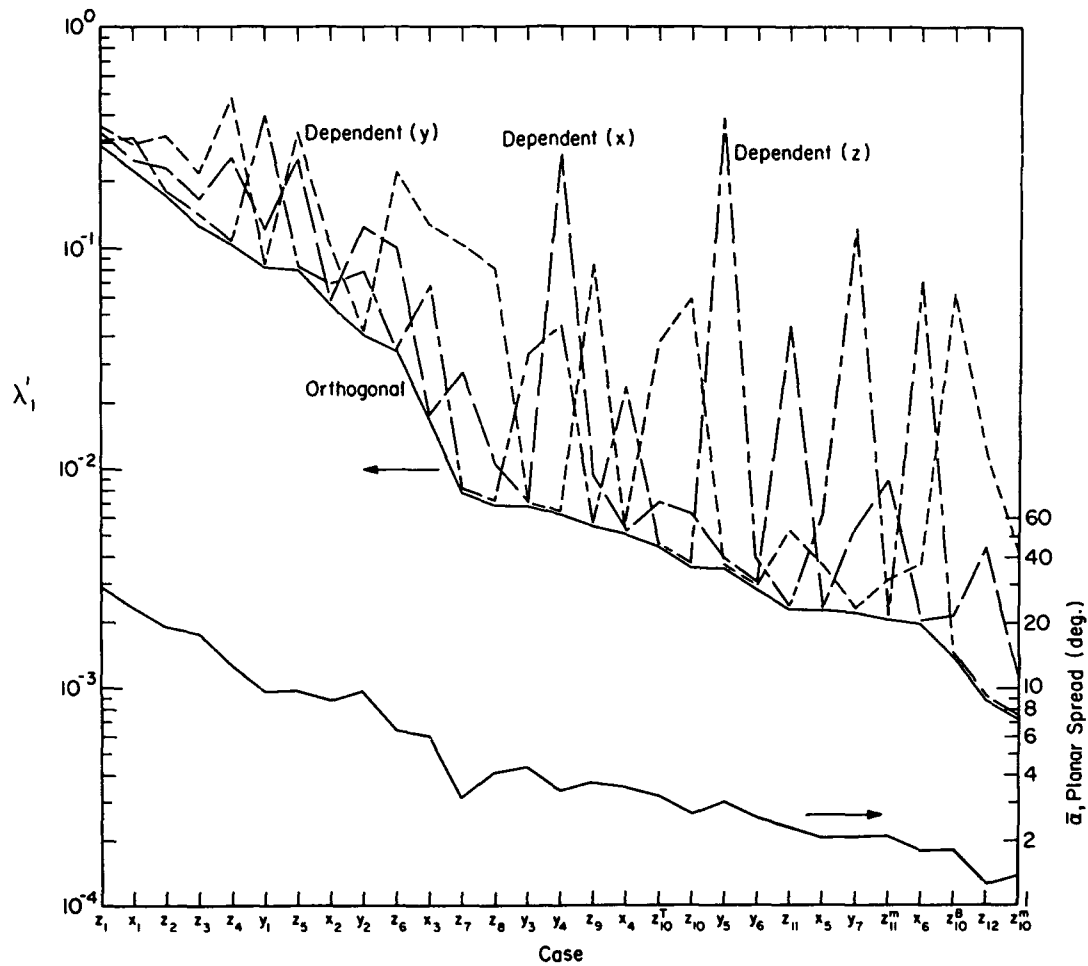
Figure 6. Mean squared normal error for several sea ice samples from orthogonal and x-, y- and z-dependent variable least-squares analyses. Planar spread from the best plane is given for these same cases. The cases are arranged arbitrarily according to λ_1 of the orthogonal analysis and named in sequence according to the best dependent-variable solution.
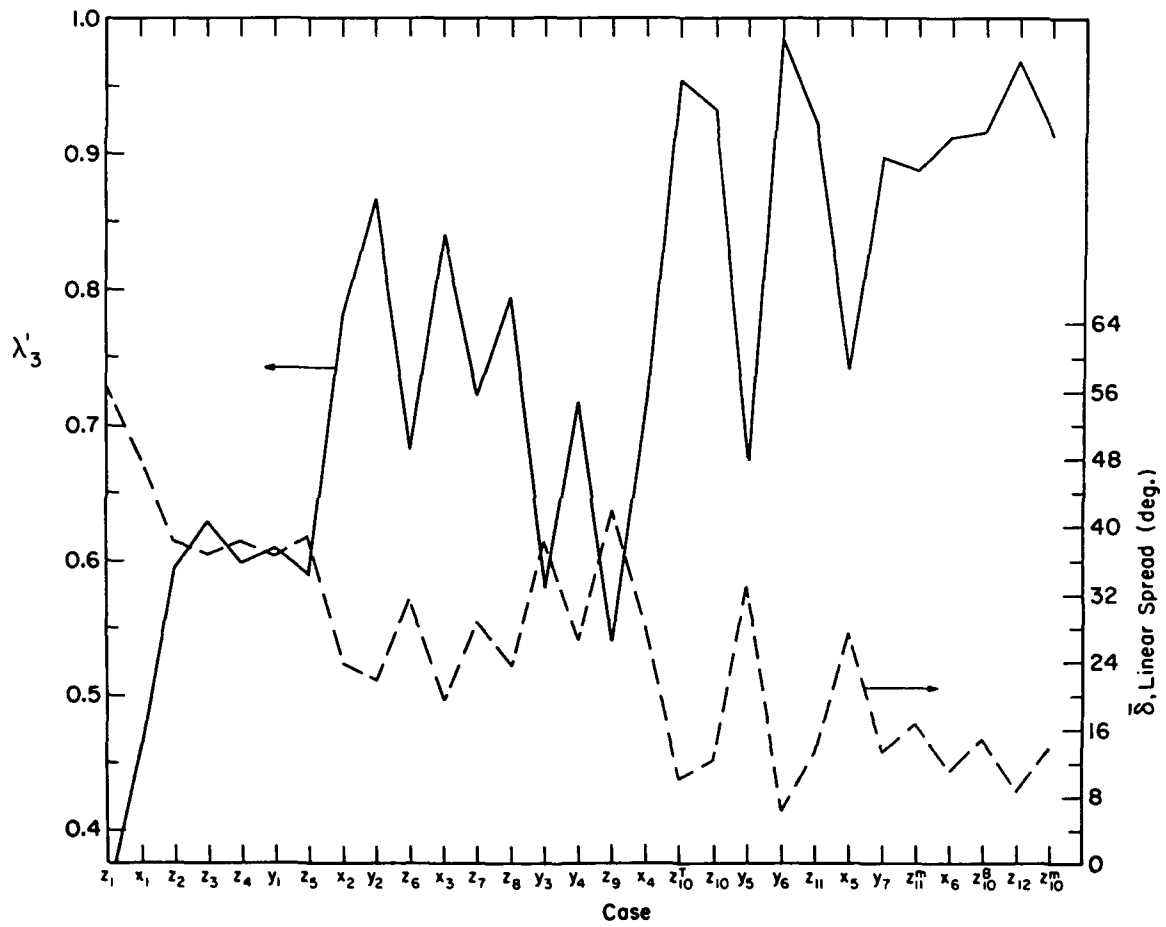
Figure 7. Maximum normalized eigenvalue and linear spread in degrees for several sea ice samples. The order and labeling of the cases is the same as in Figure 6.

13

z_1

z_{10}^T

z_{11}
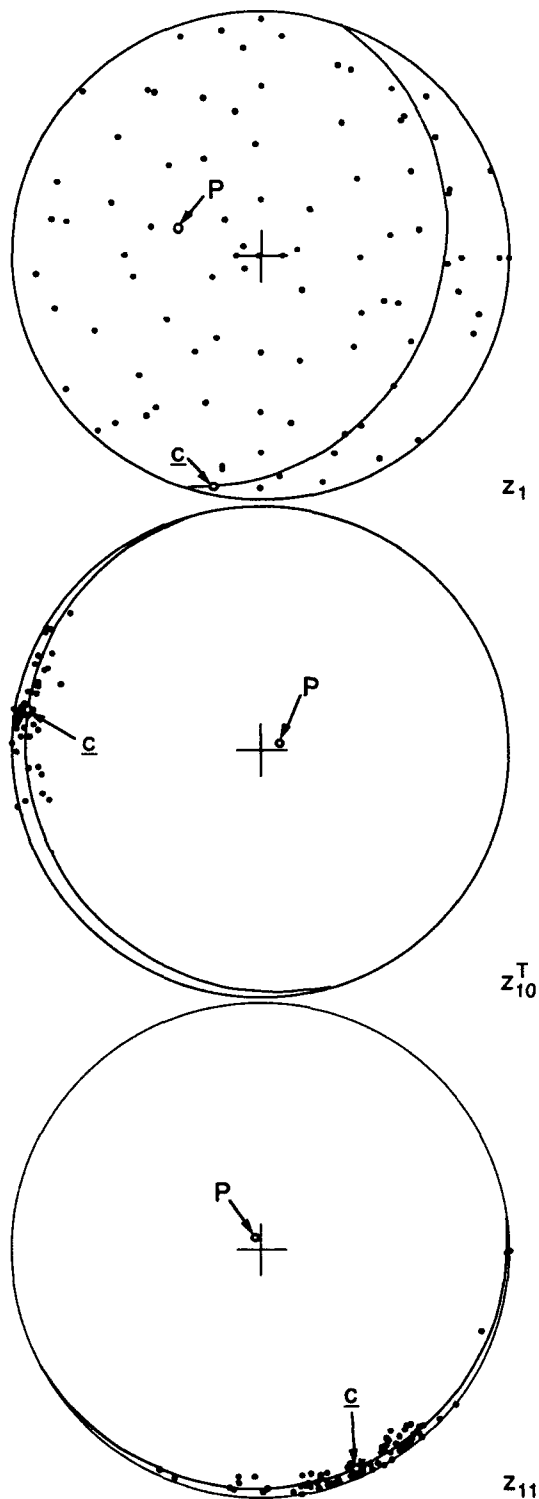
Figure 8. Schmidt net plots of cases z_1, z_{10}^T and z_{11} including the intersections with the hemisphere of the best plane, the pole P of this plane, and the best vector c.

sea ice fabrics do not necessarily correspond to the degree of preferred alignment.

Schmidt net plots of the data representing cases z_1, z_{10}^T and z_{11} are presented in Figure 8. and parameters developed from these data are given in Table 1. Included on each net are the intersections with the hemisphere of the plane of best fit, the pole P of this plane, and the vector c of best linear fit. As required, the best line is always contained in the best plane. In case z_1 the normalized eigenvalues are approximately equal, the planar and linear spreads are large, and the matrix A is nonsingular. These conditions indicate that the data are uniformly distributed over the surface of the sphere. Cases z_{10}^T and z_{11} are very different from z_1, but are similar to each other. For this group of samples λ_1' is smallest for z_{11}, indicating that these data are the most closely represented by a plane. Sample z_{10}^T has the smallest λ_2' value together with a small λ_1' and is the most linear case in this group. The distribution of data indicated by the eigenvalues is confirmed by the angles that quantify the planar and linear spreads $\overline{\alpha}$ and $\overline{\delta}$, respectively, for each sample. The matrix A is nearly singular in the latter two cases as $\lambda_1' \approx 0$ and the condition number is large.

A group of samples taken in close proximity and from the same vertical position in the ice sheet should have similar structure. Together the individual and collective analyses of these samples provide quantitative measures of comparison that indicate the sample size needed to represent the ice fabric at that location. Three samples designated $z_{10}^T, z_{10}^M, z_{10}^B$ were taken from an ice core at 1.3 m from the surface. The Schmidt net plots of both the data and the computed fits are presented in Figure 8 for z_{10}^T and in Figure 9 for the other samples and the composite data. Each of these cases has nearly the same planar structure, pole and linear structure. This similarity is quantified by the eigenvalues, planar spreads and linear spreads given in Table 1.

All the Schmidt nets presented above have been standard, depicting the lower hemisphere on the xy-plane. Alternative Schmidt nets are obtained for the hemispheres below the best fit and predominant basal planes using eq 57 and a P matrix with different eigenvector placement in each case. As a result of these transformations the position of the data on the net shifts, correcting for sample preparation error and allowing a visual assessment of the distances from the points to the best line and plane. Figure 10 gives the xy and the alternative nets for sample z_{10}^T. The data are near the perimeter of the net in the standard xy-plot. The net in the best plane corrects the sample preparation error and displays a balanced distribution of data on opposite sides of the net. The net in the basal plane depicts the points as a single group near the center of the net where linear distance is accurately represented and the linear and

14

z_{10}^M

z_{10}^B

z_{10}
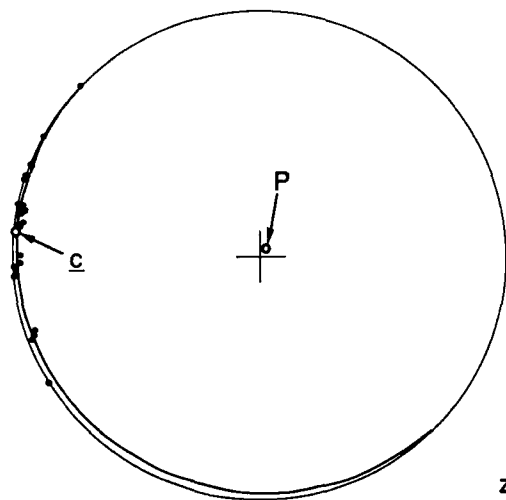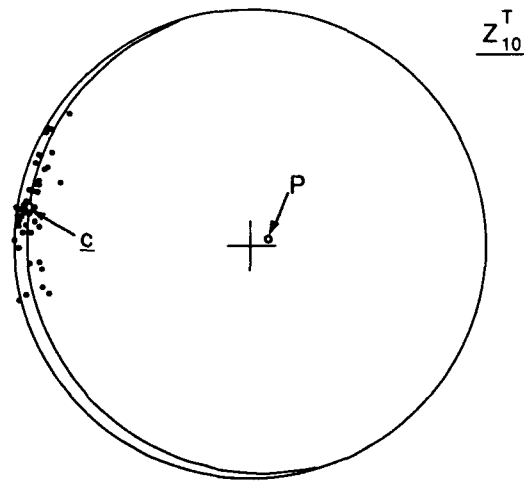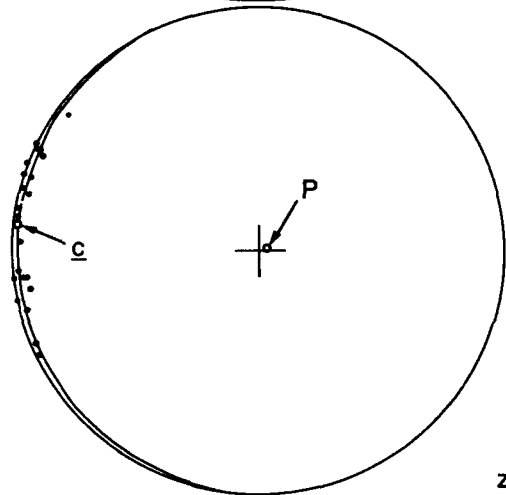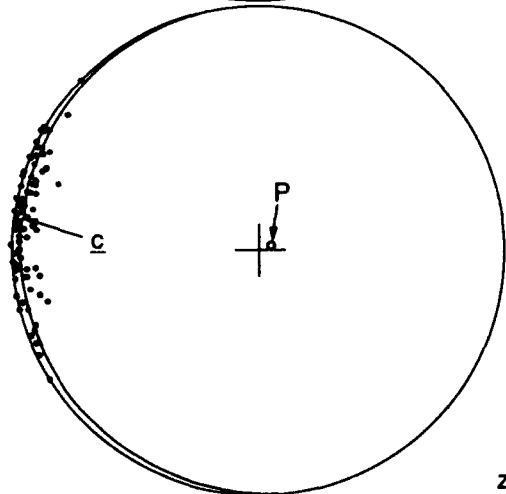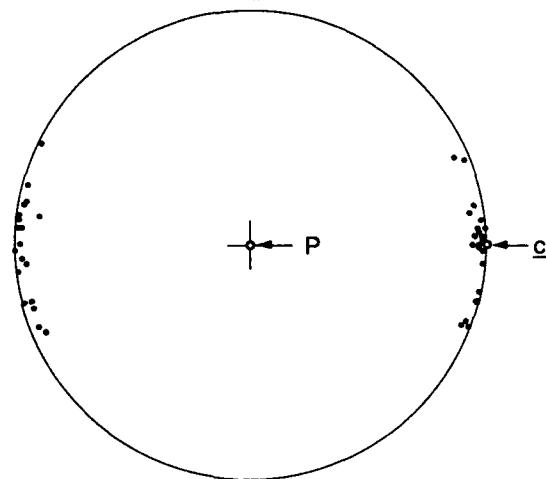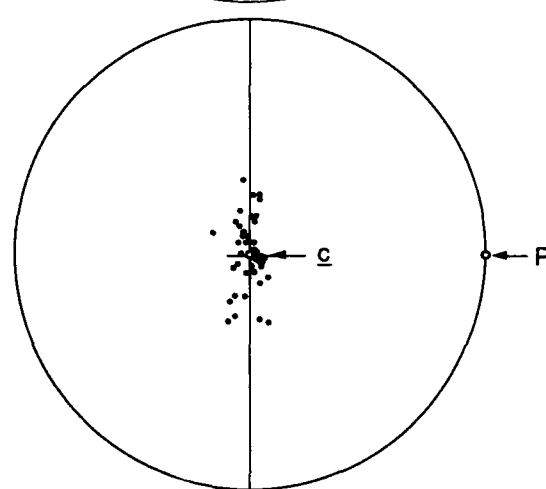
$\underline{Z}_{10}^T$

Figure 9. Schmidt net plots of cases z_{10}^M, z_{10}^B and composite case z_{10} including the intersections with the hemisphere of the best plane, the pole P of this plane, and the best vector c.

Figure 10. Schmidt net plots of case z_{10}^T in the standard xy-plane with the z-axis vertical, in the best plane with n vertical, and in the predominant basal plane with c vertical.

Table 1. Normalized eigenvalues and condition number of matrix A, and planar and linear spread of the data for selected cases. The type of the distribution is interpreted from these parameters.

Case	N	λ_1'	λ_2'	λ_3'	$\bar{\alpha}$ (deg)	$\bar{\delta}$ (deg)	Cond(A)	Type of distribution
z_1	90	0.2940	0.3510	0.355	29.3	56.4	1.21	Uniform
z_{11}	77	0.00235	0.0755	0.922	2.3	13.5	392	Planar/linear
$\bar{z}_{10}$	44	0.00452	0.0417	0.954	3.2	10.4	211	Linear/planar
z_{16}	22	0.00073	0.0863	0.913	1.4	14.2	1250	Planar/linear
$\bar{z}_{10}$	23	0.00140	0.0813	0.917	1.8	14.9	653	Planar/linear
z_{10}	89	0.00359	0.0638	0.933	2.7	12.5	260	Planar/linear

planar fits can be readily evaluated and compared to other samples.

CONCLUSIONS

A quantitative characterization of ice fabrics is critical for understanding the mechanical properties of sea ice, but was not previously available. An orthogonal least-squares analysis of uniaxial crystal orientation data was developed from geometric arguments with unit vectors representing individual crystal orientations. Minimization of the perpendicular distances with a best line or plane provided an eigenvalue problem that was identical to that obtained by other investigators using different methods. Normalized eigenvalues give the mean squared normal distance of the data from the line or plane, and corresponding eigenvectors provide the dominant c-axis, planar, and basal plane orientations, and the direction of columnar crystal elongation. The preferred c-axis orientation is always contained in the plane of best fit. The method is the basis of a relatively simple algorithm for computer analysis of large volumes of orientation data.

The formulation of a least-squares method greatly influences the results. This observation was demonstrated for many samples of first-year sea ice by comparing the mean squared normal distance of the data with planes obtained using the classical dependent variable least-squares approaches and the orthogonal method. The dependent-variable solutions produced dramatically different planes of best fit with erratic and widely varying normal errors. The error approached the minimum given by the orthogonal method when the dependent variable direction was almost normal to the best plane. Orthogonal least-squares and other analogous methods producing the eigenvalue problem all rely on the implicit assumption of equal measurement error in all coordinate directions at all points on the unit sphere. We find that this assumption is a first approximation for optical data obtained with the universal stage.

Normalized eigenvalues give the mean squared normal distance between the data on the unit sphere and the plane through the origin normal to the corresponding eigenvector. This measure of the planar fit to data is equivalent to the variance in classical dependent variable least-squares methods. The majority of the sea ice samples studied had planar fabrics, and several had aligned fabrics, characterized by mean squared normal distances of less than 0.1 with the data. These relative distances are well represented by the angular measures of linear and planar spread; however, the distance and angular error measures are not equivalent. For these samples increasingly planar orientations of the c-axes do not correspond to increasingly linear fabrics.

The normalized eigenvalues allow quantitative comparisons between samples, and of composite data representing a collection of several samples. Proximate samples from the same vertical position in the ice sheet had nearly identical structure. This similarity, quantified by the computed eigenvalues and eigenvectors, was displayed on Schmidt nets for the individual samples and the composite. The capability to view the data and the analytical results on Schmidt nets in the planes defined by the eigenvectors was developed, providing information to improve the interpretation of the data and the fits by minimizing the importance of sample preparation, net distortion, and measurement accuracy limitations.

The eigenvalue/eigenvector analysis has been applied to fabrics displaying other patterns, including multi-maxima and small circle girdles. Fitting these data with a best line or plane yields results that can only

be qualitatively interpreted. However, when a fabric displays several point maxima it may be possible to objectively subdivide the data. The best line for each subset would quantify the orientation and alignment of the corresponding point maximum. The intersection of cones with orientation diagrams were drawn by Kohnen and Gow (1979) to bound small circle girdle fabrics. A small circle girdle fabric could be assessed quantitatively by finding a circular cone with its axis defined by the best line and its apex at the origin. The surface of the cone would be located to minimize the sum of the squared distances with the data, and variability measures could again be defined in terms of distance and angle.

LITERATURE CITED

Beyer, W.H. (1987) *Handbook of Mathematical Sciences,* 6th Edition, CRC Press, Inc., Boca Raton, FL.

Diggle, P.J. and N.I. Fisher (1985) Sphere: A contouring program for spherical data, *Computers & Geosciences,* Vol. 11(6), pp. 725–766.

Fairbairn, H.W. (1949) *Structural Petrology of Deformed Rocks,* Addison-Wesley Publishing Company, Inc., Cambridge, MA.

Herron, S.L. and C.C. Langway, Jr. (1982) A comparison of ice fabrics and textures at Camp Century, Greenland and Byrd Station, Antarctica, *Annals of Glaciology,* Vol. 3, pp. 118-124.

Hildebrand, F.B. (1965) *Methods of Applied Mathematics,* 2nd Edition, Prentice-Hall, Englewood Cliffs, NJ.

Kamb, W.B. (1962) Refraction corrections for universal stage measurements I. Uniaxial crystals, *The American Mineralogist,* Vol. 47, March–April, pp. 227–245.

Kass, S. (1989) Spaces of closest fit, *Linear Algebra and Its Applications,* Vol. 117, pp. 93–97.

Knopf, E.B. and E. Ingerson (1938) *Structural Petrology,* Geological Society of America Memoir 6.

Kohnen, H. and A.J. Gow (1979) Ultrasonic velocity investigations of crystal anisotropy in deep ice cores from Antarctica, USA Cold Regions Research and Engineering Laboratory, CRREL Report 79-10.

Langway, C.C., Jr. (1958) Ice fabrics and the universal stage, U.S. Army Snow, Ice and Permafrost Research Establishment Tech. Report 62, available from USACRREL, 16 pp.

Mardia, K.V. (1972) *Statistics of Directional Data,* Academic Press, New York, pp. 212–286.

Pearson, K. (1901) On lines and planes of closest fit to systems of points in space, *Philos. Mag. 6th Ser.,* Vol. 2(11), pp. 559–572.

Reed, B.C. (1989) Linear least-squares fits with errors in both coordinates, *American Journal of Physics,* Vol. 57(7), pp. 642–646.

Richter-Menge, J.A., G.F.N. Cox and N.M. Perron (1987) Mechanical properties of multi-year sea ice, Phase I: Ice structure analysis, USA Cold Regions Research and Engineering Laboratory, CRREL Report 87-3.

Shields, P.C. (1968) *Elementary Linear Algebra,* Worth Publishers, Inc., New York.

Turner, F.J. and L.E. Weiss (1963) *Structural Analysis of Metamorphic Tectonites,* McGraw-Hill Book Company, Inc., New York.

Wang, Y.S. (1979) Crystallographic studies and strength tests of field ice in the Alaskan Beaufort Sea, POAC 79, *In* Proceedings of the Fifth International Conference on Port and Ocean Engineering under Arctic Conditions. Vol. 1, pp. 651–665.

Watson, G.S. (1966) The statistics of orientation data, *Journal of Geology,* Vol. 74(5), pp. 786–797.

Weeks, W.F. and S.F. Ackley (1982) The growth, structure and properties of sea ice, USA Cold Regions Research and Engineering Laboratory, CRREL Monograph 82-1.

Weeks, W.F. and A.J. Gow (1978) Preferred crystal orientations along the margins of the Arctic Ocean, *Journal of Geophysical Research,* Vol. 84, pp. 5105–5121.

REPORT DOCUMENTATION PAGE

Public reporting burden for this collection of information is estimated to average 1 hour per response, including the time for reviewing instructions, searching existing data sources, gathering and maintaining the data needed, and completing and reviewing the collection of information. Send comments regarding this burden estimate or any other aspect of this collection of information, including suggestion for reducing this burden, to Washington Headquarters Services, Directorate for Information Operations and Reports, 1215 Jefferson Davis Highway, Suite 1204, Arlington, VA 22202-4302, and to the Office of Management and Budget, Paperwork Reduction Project (0704-0188), Washington, DC 20503.

1. AGENCY USE ONLY (Leave blank)	2. REPORT DATE	3. REPORT TYPE AND DATES COVERED
	March 1992	

4. TITLE AND SUBTITLE

Vector Analysis of Ice Fabric Data

5. FUNDING NUMBERS

PE: 6.11.02A
PR: 4A161102AT24
TA: SS
WU: 001

6. AUTHORS

Michael G. Ferrick and Kerran J. Claffey

7. PERFORMING ORGANIZATION NAME(S) AND ADDRESS(ES)

U.S. Army Cold Regions Research and Engineering Laboratory
72 Lyme Road
Hanover, N.H. 03755-1290

8. PERFORMING ORGANIZATION REPORT NUMBER

CRREL Report 92-1

9. SPONSORING/MONITORING AGENCY NAME(S) AND ADDRESS(ES)

Office of the Chief of Engineers
Washington, D.C. 20314

10. SPONSORING/MONITORING AGENCY REPORT NUMBER

11. SUPPLEMENTARY NOTES

12a. DISTRIBUTION/AVAILABILITY STATEMENT

Approved for public release; distribution is unlimited.

Available from NTIS, Springfield, Virginia 22161.

12b. DISTRIBUTION CODE

13. ABSTRACT (Maximum 200 words)

The mechanical properties of ice are strongly affected by crystal texture and c-axis alignment. In this report we develop a general quantitative method for analysis of uniaxial crystal orientation data. These data are represented as unit vectors from the origin with endpoints on the surface of a unit sphere. An orthogonal least-squares error measure is used to develop equations that define the closest plane and line through the data. The resulting eigenvalue problem is identical to that obtained by other investigators using different methods. However, we identify an implicit assumption in the method, and observe that the error measure represents physical distance and quantifies the goodness-of-fit of the idealized structures to the data. For comparison, a parallel development is presented of classical dependent-variable least squares. A method is developed to transform the data and the results for viewing on Schmidt nets drawn in the best plane and the predominant basal plane of a sample, in addition to the standard xy-plane. Applications of the analysis to sea ice samples include both numerical and Schmidt net presentations of results.

14. SUBJECT TERMS

c-axis orientation	Orthogonal least-squares	Sea ice
Crystal fabric analysis	Schmidt nets	

15. NUMBER OF PAGES
23

16. PRICE CODE

17. SECURITY CLASSIFICATION OF REPORT	18. SECURITY CLASSIFICATION OF THIS PAGE	19. SECURITY CLASSIFICATION OF ABSTRACT	20. LIMITATION OF ABSTRACT
UNCLASSIFIED	UNCLASSIFIED	UNCLASSIFIED	UL

NSN 7540-01-280-5500

Standard Form 298 (Rev. 2-89)
Prescribed by ANSI Std. Z39-18
298-102